drones

MDPI

Article

The Provision of Physical Protection of Information During the Transmission of Commands to a Group of UAVs Using Fiber Optic Communication Within the Group

Dina Shaltykova [1], Aruzhan Kadyrzhan [1,2], Yelizaveta Vitulyova [3,4,5,*] and Ibragim Suleimenov [1,3,5]

[1] National Engineering Academy of the Republic of Kazakhstan, Almaty 050060, Kazakhstan; shaltykova.d@mail.ru (D.S.); aru.kadyrzhan@gmail.com (A.K.); esenych@yandex.kz (I.S.)
[2] Institute of Communications and Space Engineering, Gumarbek Daukeev Almaty University of Power Engineering and Communications, Almaty 050040, Kazakhstan
[3] National Scientific Laboratory for the Collective Use of Information and Space Technologies (NSLC IST), 22 Satbayev Street, Almaty 050013, Kazakhstan
[4] JSC "Institute of Digital Engineering and Technology", Almaty 050000, Kazakhstan
[5] Department of Smart Technologies in Engineering, International Engineering and Technological University, Almaty 050060, Kazakhstan
* Correspondence: lizavita@list.ru

Highlights

What are the main findings?

- The report introduces a geometric method for unambiguous localization of remote radio-signal sources using three UAVs connected by fiber-optic links, relying on the intersection of hyperbola asymptotes rather than full hyperbola curves.
- It proves that the physically correct emitter location is always the asymptote-intersection point farthest from the UAV formation center, while all spurious solutions remain confined near the formation radius.

What are the implications of the main findings?

- The method enables secure, interference-resistant command transmission from the operator to the UAV group and supports the detection of external radio emitters (including operators and electronic-warfare systems) under line-of-sight conditions.
- The approach provides a scalable foundation for expanding UAV groups with nodes using directional antennas and lightweight protection mechanisms, supporting resilient architectures and advanced configurations such as jet-assisted UAV platforms.

Abstract

This paper presents a novel method for the precise localization of remote radio-signal sources using a formation of unmanned aerial vehicles (UAVs). The approach is based on time-difference-of-arrival (TDoA) measurements and the geometric analysis of hyperbolas formed by pairs of UAVs. By studying the asymptotic intersections of these hyperbolas, the method ensures unique determination of the source position, even in the presence of multiple intersection points. Theoretical analysis confirms that the correct intersection point is located at a significantly larger distance from the UAV formation center compared to spurious intersections, providing a rigorous criterion for resolving localization ambiguity. The proposed framework also addresses secure inter-UAV communication via optical-fiber links and supports expansion of UAV groups with directional antennas and low-power signal relays. Additionally, the study discusses practical UAV configurations, including hybrid propulsion and jet-assisted kamikaze platforms, demonstrating the applicability of the method in contested environments. The results indicate that this approach provides

Received: 23 November 2025
Revised: 25 December 2025
Accepted: 31 December 2025
Published: 1 January 2026

a robust mathematical basis for unambiguous emitter localization and enables scalable, secure, and resilient multi-UAV systems, with potential applications in electronic-warfare scenarios, surveillance, and tactical operations.

Keywords: information protection; UAV; hyperbolic asymptotes; optical fiber; data obfuscation; onboard computing systems

1. Introduction

Unmanned aerial vehicle (UAV) groups are increasingly used to address a wide range of tasks, including remote sensing [1,2]. They are employed for monitoring agricultural [3,4] and forested [5] areas, as well as for environmental surveillance [6,7]. The relevance of operating UAVs in group mode requires no extensive justification. A group, understood as a system whose elements are connected through communication channels, can continue performing a designated task even when some of its elements are lost [8,9]. The use of UAV groups also reduces the required number of operators [10,11], which becomes increasingly important as the total number of UAVs deployed for various purposes continues to grow. This trend is particularly evident in military applications [12–14]. As emphasized in [15], it is to be expected that there will be a transition from the currently used UAV types controlled by a single operator to UAV swarms [16] designed to create mobile networks covering large areas and enabling communication between small military units. Moreover, such groups are already being equipped with artificial intelligence (AI) for military use [17]. The potential for integrating UAV groups with AI is becoming increasingly clear [18–20]. These developments inevitably bring attention to several issues actively discussed in the current literature. One of these issues is the improvement of algorithms for UAV group (swarm) control [21–23]. Equally important is the problem of information security [24,25], particularly the mitigation of communication attacks [26,27]. As noted in [14], methods involving cryptography are widely used for this purpose [28,29].

However, the application of such methods faces well-defined limitations. First, methods for remote information interference with UAVs continue to advance [30,31], and the increasing complexity of swarm architectures [32,33] inevitably introduces additional vulnerabilities. Second, data leaks related to human factors may occur. For this reason, during the current armed conflict in Ukraine, UAVs controlled via fiber-optic data transmission—whose length is continuously increasing and, according to open sources, now exceeds several kilometers—are being used with increasing frequency; meanwhile, the military tactics of UAV deployment are also continuously evolving [34,35]. This method is inherently the most reliable for preventing external interference, but it is associated with considerable technical challenges, particularly the weight requirements for fiber-optic cable whose length may reach ten kilometers or more.

These challenges bring renewed attention to the problem formulation presented in [36–38], namely, ensuring information protection by physical means without relying on long fiber-optic communication lines. This problem was largely addressed in our previous work [15], where the idea initially proposed in [39] was further developed. Specifically, ref. [39] demonstrated that information protection can be ensured by determining the coordinates of the signal source. This approach is applicable primarily within the line-of-sight (LoS) region, but considering typical UAV deployment scenarios—including military ones—it has direct practical relevance [15]. In that work, it was shown that the coordinates of a signal source can be determined using three UAVs interconnected with fiber-optic data links. This enables source identification based on the “friend or foe” principle. The use

of three UAVs corresponds to the classical problem of determining the coordinates of a signal source based on time-delay measurements, which reduces to solving a system of second-degree algebraic equations [40]. The solution corresponds to finding the intersection points of hyperbolas, whose governing parameter includes the recorded time delay.

In the present study, this problem is analyzed in detail. It is shown that one may select a coordinate system complementary to the method proposed in [15]. We demonstrate that the specifics of this method allow one to reduce the task to finding the intersection of the asymptotes of these hyperbolas with satisfactory accuracy. Particular attention is paid to the uniqueness of the resulting solution, which ensures the correct determination of the signal source coordinates. The potential use of the proposed system as a relay for transmitting commands to additional UAVs within the group is also discussed.

2. Related Works

The system considered in this work is based on measuring the difference in the signal propagation time from a source to two UAVs forming a pair. Solving this problem requires time synchronization (SYNC) of the onboard units of the UAVs. Similar problems have been addressed in numerous studies, including [41–43]. An advantage of using fiber-optic links between the UAVs in a group is that time synchronization is significantly simplified [15], because signal transmission over fiber eliminates the impact of external signals and, most importantly, the distance between the UAVs is known a priori, since the fiber length can be fixed by independent means, including mechanical methods.

For this task, it is also important to discuss the issue of time difference of arrival (TDoA) accuracy, which is examined in the literature from various perspectives [44,45]. This issue is closely related to the positioning problem for robotic vehicles, which is likewise discussed in current research from different angles [46–48]. In most cases, the objective is to improve the accuracy of estimating the coordinates of a vehicle, a radio-signal source, and related targets. Achieving high positioning accuracy is also the goal of adjacent research directions, such as acoustic-based methods [49,50] and indoor positioning [51,52]. However, in the context of the present work, the positioning-accuracy question lies in a somewhat different domain, because there exist practical tasks for which positioning can be performed with intentionally reduced accuracy.

The use of UAV groups also often entails addressing the swarm synchronization problem [53,54]. Such synchronization implies that autonomous agents within a group coordinate their behavior in time and/or space so as to act as a single entity, without centralized control (or with minimal central control). The proposed approach, however, makes it possible to bypass this problem by leveraging geometric factors. As will be shown below, the method remains operational for any mutual configuration of the employed UAVs.

From the perspective of the objectives of this study, the research reported in the literature and devoted to the problem of determining the coordinates of a signal source (or, equivalently, the direction to the signal source) can be classified as follows:

- determining the signal source coordinates by measuring time delays (TDoA) [40,44];
- determining these coordinates by using antennas with a sufficiently narrow radiation pattern (high directivity) [55];
- determining these coordinates by measuring the received signal level (RSS-based approaches) [56].

All of these methods are well known and have been extensively validated, including in practical applications. However, from the standpoint of information protection based on a UAV group intended to operate in a line-of-sight (LoS) environment, each of them exhibits specific limitations.

Specifically, the first group of methods inherently requires information exchange between spatially separated receivers [41–43]. For UAV-based applications, the communication channels enabling such exchange (especially when operator localization is used as part of an information protection mechanism) must themselves be maximally secure. Maximum protection is clearly achieved by employing a communication line that minimizes the possibility of external informational interference. This requirement is satisfied by fiber-optic communication. As demonstrated by the experience of the ongoing military conflict in Ukraine, fiber-optic control of drones has proven to be sufficiently effective despite the limited length of such links. However, the use of fiber-optic lines with lengths on the order of a kilometer or more faces well-defined practical challenges. Our approach makes it possible to reduce the required fiber length to hundreds of meters or less. The fundamentally novel aspect of our approach is the choice of a coordinate system that is maximally convenient for solving the stated problem. This choice is explicitly oriented toward a group of three UAVs interconnected by fiber-optic links.

The second group of methods also has a pronounced drawback for the problem addressed in this work: the cost and implementation complexity of such antennas increase substantially as their performance characteristics are improved [57]. The main difficulty in applying them to UAVs is that the vehicle receiving the operator's signal must be oriented appropriately in space, which is not always feasible.

Methods based on measuring the signal level [58] primarily allow one to estimate the range to the signal source (operator), which is not suitable for solving the problem considered in this paper.

Based on the above, an information protection method built around fiber-optic communication lines offers advantages for the target class of tasks—namely, protecting information transmitted from an operator to a UAV group within line-of-sight conditions.

3. Methods

The study primarily employs analytical methods for solving the equations used to determine the operator's coordinates based on the known positions of three UAVs and the time-of-arrival (TOA) differences of a signal emitted by the operator. The possibility of obtaining an analytical solution is enabled by considering the intersections of the hyperbolas' asymptotes rather than the intersections of the hyperbolas themselves. It is demonstrated that the coordinate-estimation accuracy provided by this approach is sufficient for practical use in protecting information within a line-of-sight communication zone.

The conclusions derived from the analytical developments are supported by computer-based experiments. In these experiments, an algorithm was implemented based on the analytical derivations presented in the paper; the code is provided in the Supporting Materials. In the first series of experiments, the intersection points of the hyperbolas were computed using the developed code and compared with the true position of the signal source. The results are presented in the form of figures and a table. In the second series of experiments, the influence of errors in determining the TOA differences on the estimation of the operator's coordinates was investigated. The results are presented as figures that clearly illustrate the discrepancy between the apparent and the true position of the operator (signal source).

4. Results

The implementation scheme of the method proposed in [15] is shown in Figure 1. The diagram illustrates the minimal number of UAVs required to apply the method—namely, three. These three UAVs form two pairs, and for each pair, the time-of-arrival (TOA)

difference of a signal emitted by a common source and received by the onboard receivers is measured as Δt_{12} and Δt_{23}.

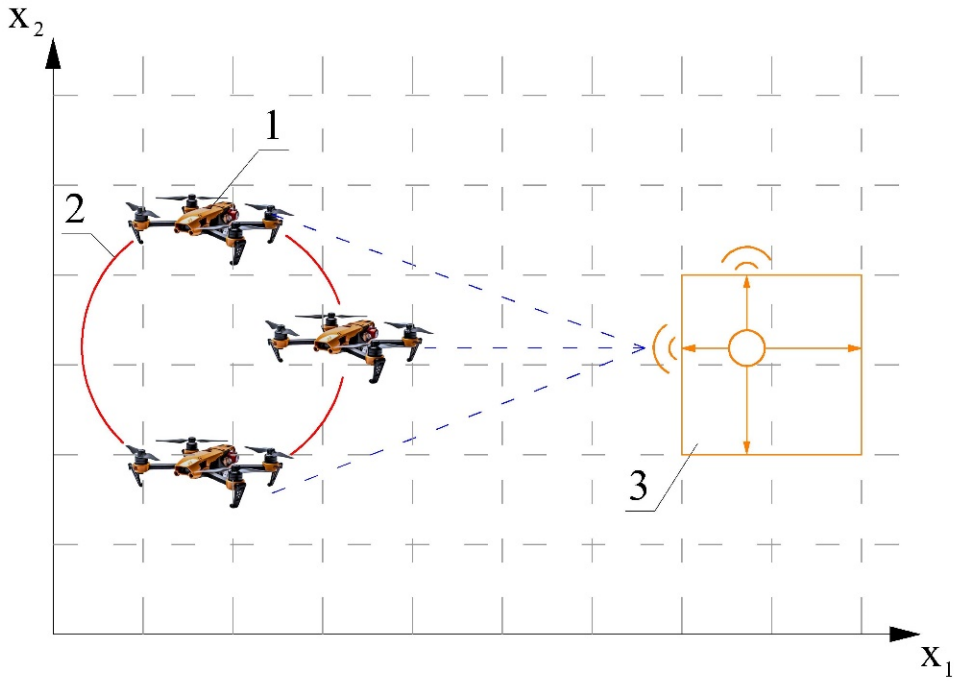

Figure 1. Scheme of the information-protection method using fiber-optic communication within a UAV group; 1—UAV, 2—fiber-optic communication lines (schematically), 3—signal (command) source.

If the problem can be reduced to a two-dimensional one (i.e., the altitude coordinate is neglected), then the measurement Δt_{12} corresponds to identifying a curve (a hyperbola) described by

$$r_1 - r_2 = c\Delta t_{ij} \quad (1)$$

where

$r_{1,2} = \sqrt{(\vec{r} - \vec{r}_{10,20})^2}$,

$\vec{r}_{10,20}$ are the radius vectors of the receiving units on the UAVs,

$\vec{r} = (x, y)$ is the current radius vector,

c is the speed of light, and

Δt_{ij} is the difference in signal propagation time from the source to UAVs i and j.

Using two receiver pairs corresponds to using two equations of type (1), so the source coordinates can be determined as the intersection point of two hyperbolas defined by such equations, which is consistent with the classical time-difference-of-arrival (TDoA) method described, for example, in [40].

From the perspective of external attacks, vulnerabilities may arise during the formation of communication channels between the UAVs in the group. Fiber-optic communication minimizes these risks [15]. Moreover, it provides additional opportunities for synchronization between the computational units that determine Δt_{12} and Δt_{23}. The specific scheme implementing the measurement of these delays based on the phase-portrait method is presented in [15].

Owing to the use of fiber optics, synchronization is implemented in a straightforward manner. On the transmitter side, a single digital SYNC pulse is generated and simultaneously delivered via the fiber-optic link to all receiving modules. The optical receiver converts the optical pulse into a 3.3 V digital signal, which is applied to the microcontroller timer input. As a result, the same rising edge of the SYNC signal is hardware-captured by all elements of the group with minimal time spread, determined only by the delay of the

optical transceiver and the timer input logic. The synchronization error (time resolution) when using this approach together with the phase-portrait method does not exceed 5% [15]. This value was therefore adopted in the computer experiments reported below.

We also emphasize that the concept of using fiber optics to form a UAV group capable of determining the location of a radio-signal source was first discussed systematically in [15], and was initially proposed in our earlier work [59] (although without substantial elaboration).

One advantage of the phase-portrait method [15] is that the time delay can be detected using a single fragment of a modulated harmonic oscillation.

However, report [15] did not address several accompanying geometric problems, which are resolved in the present study. In particular, we show that the correct solution can be uniquely selected based on physical considerations.

To ensure uniform treatment of all three UAVs—the minimal number required to determine the location of the signal source—the coordinate system used in what follows is chosen such that its origin coincides with the center of the circle passing through the three UAV positions. Although finding such a circle is an elementary trigonometric problem, we detail the construction due to its importance.

Three points (x_1, y_1), (x_2, y_2), and (x_3, y_3) lie on a circle of radius ρ_0 if the following relations hold:

$$\begin{aligned} (x_1 - x_0)^2 + (y_1 - y_0)^2 &= \rho_0^2 \\ (x_2 - x_0)^2 + (y_2 - y_0)^2 &= \rho_0^2 \\ (x_3 - x_0)^2 + (y_3 - y_0)^2 &= \rho_0^2 \end{aligned} \tag{2}$$

where (x_0, y_0) are the unknown coordinates of the circle center.

This system reduces to a linear one. Expanding the terms in (2) and subtracting the third equation from the first two yields:

$$2(x_1 - x_2)x_0 + 2(y_1 - y_2)y_0 = R_1^2 - R_2^2 \tag{3}$$

$$2(x_3 - x_2)x_0 + 2(y_3 - y_2)y_0 = R_3^2 - R_2^2 \tag{4}$$

where $R_i^2 = x_i^2 + y_i^2$.

Equations (3) and (4) constitute a linear system that enables computing the circle center, after which all vectors can be transformed into this new coordinate system. These equations correspond to the classical geometric construction used to locate the center of a circle defined by three given points.

From this point onward, all calculations are carried out in this coordinate system, where the origin coincides with the center of the circle passing through the three UAVs.

Geometrically, the problem reduces to finding the intersection of two hyperbolas, each generated by the TOA (or phase-difference) measurement from a separate UAV pair. Indeed, the phase difference $\Delta\phi$ (measured according to [15]) is related to the difference in distances between the signal source and UAVs 1 and 2 by

$$r_1 - r_2 = cT\frac{\Delta\phi}{2\pi} = R \tag{5}$$

where T is the signal period, where $r_{1,2} = \sqrt{\left(\vec{r} - \vec{r}_{10,20}\right)^2}$, $\vec{r}_{10,20}$ are the radius vectors of the receivers, $\vec{r} = (x, y)$ is the current radius vector, c is the speed of light, and T is the period of the transmitted signal. It is essential that, due to the specifics of the problem under consideration, all vectors can be assumed to lie in a plane.

We emphasize that Equation (5), when expressed in terms of the current radius vector, represents the equation of a hyperbola; that is, one UAV pair generates one hyperbola (consisting of two branches). A second UAV pair yields another hyperbola. One of the intersection points of these curves corresponds to the location of the radio signal source. The non-uniqueness of this geometric solution requires additional analysis. As will become evident below, a unique solution can indeed be obtained due to the structure of the problem.

Let us transform Equation (5) to polar coordinates associated with the chosen coordinate origin. After straightforward algebra, we obtain

$$(4\rho\rho_0)^2\sin^2\frac{\varphi_2-\varphi_1}{2}\sin^2\left(\varphi-\frac{\varphi_2+\varphi_1}{2}\right)+8\rho\rho_0R^2\cos\frac{\varphi_2-\varphi_1}{2}\cos\left(\varphi-\frac{\varphi_2+\varphi_1}{2}\right)-4R^2\left(\rho^2+\rho_0^2\right)+R^4=0 \quad (6)$$

where the standard formulas for converting to polar coordinates were used. The current radius vector is written as

$$\vec{r}=\rho(\cos\varphi,\sin\varphi) \quad (7)$$

and the coordinates of UAVs 1 and 2 are given by

$$\vec{r}_{10,20}=\rho_0(\cos\varphi_{1,2},\sin\varphi_{1,2}) \quad (8)$$

To verify Equation (6), consider the limiting case corresponding to the canonical form of a hyperbola in polar coordinates. Let the two UAVs lie on a straight line passing through the center of the reference circle, which coincides with the origin. In this case one may set $\varphi_1=0$, implying $\varphi_2=\pi$, so that

$$\sin\frac{\varphi_2+\varphi_1}{2}=1,\ \cos\frac{\varphi_2-\varphi_1}{2}=0 \quad (9)$$

Thus Equation (6) reduces to

$$(4\rho\rho_0)^2\cos^2\varphi-4R^2\left(\rho^2+\rho_0^2\right)+R^4=0 \quad (10)$$

since $\sin(\varphi-\pi/2)=-\cos\varphi$.

The quantities in Equation (10) can be expressed in terms of the eccentricity ε and parameter a of the canonical hyperbola

$$\frac{x^2}{a^2}-\frac{y^2}{b^2}=1 \quad (11)$$

Classical relations for conic sections yield

$$R=2a;\ \varepsilon=\sqrt{1+\frac{b^2}{a^2}}>1;\ \rho_0=\varepsilon a \quad (12)$$

where the last relation follows from the fact that the UAVs coincide with the foci of the hyperbola. Substituting (12) into (10) gives the canonical hyperbola in polar coordinates:

$$\rho^2=a^2\frac{\varepsilon^2-1}{\varepsilon^2\cos^2\varphi-1}=\frac{b^2}{\varepsilon^2\cos^2\varphi-1} \quad (13)$$

Thus Equation (6) is consistent with the known limiting case. Let us now return to the general formulation.

Introduce the dimensionless quantities

$$q=\frac{a}{\rho_0}=\frac{R}{2\rho_0};\ s=\frac{\rho}{\rho_0} \quad (14)$$

Substituting (14) into (6) yields a quadratic equation for s:

$$s^2\left[\sin^2\frac{\varphi_2-\varphi_1}{2}\sin^2\left(\varphi-\frac{\varphi_2+\varphi_1}{2}\right)-q^2\right]+2sq^2\cos\frac{\varphi_2-\varphi_1}{2}\cos\left(\varphi-\frac{\varphi_2+\varphi_1}{2}\right)-q^2+q^4=0 \quad (15)$$

Its analytical solution is

$$s_{1,2}=q\frac{-q\cos\frac{\varphi_2-\varphi_1}{2}\cos\left(\varphi-\frac{\varphi_2+\varphi_1}{2}\right)\pm\sqrt{\left(\sin^2\frac{\varphi_2-\varphi_1}{2}-q^2\right)\left(\sin^2\left(\varphi-\frac{\varphi_2+\varphi_1}{2}\right)-q^2\right)}}{\sin^2\frac{\varphi_2-\varphi_1}{2}\sin^2\left(\varphi-\frac{\varphi_2+\varphi_1}{2}\right)-q^2} \quad (16)$$

To check this expression, set $\varphi_1=0$. Then

$$s_{1,2}=q\frac{-q\cos\frac{\varphi_2}{2}\cos\left(\varphi-\frac{\varphi_2}{2}\right)\pm\sqrt{\left(\sin^2\frac{\varphi_2}{2}-q^2\right)\left(\sin^2\left(\varphi-\frac{\varphi_2}{2}\right)-q^2\right)}}{\sin^2\frac{\varphi_2}{2}\sin^2\left(\varphi-\frac{\varphi_2}{2}\right)-q^2} \quad (17)$$

Examples computed using these formulas are shown in Figure 2a,b. The plots show the dependence of the normalized ordinate $\frac{y}{\rho_0}=\frac{\rho}{\rho_0}\sin\varphi$ on the normalized abscissa $\frac{x}{\rho_0}=\frac{\rho}{\rho_0}\cos\varphi$. As expected, the solutions indeed correspond to hyperbolas whose foci lie on the unit circle, consistent with the dimensionless transformation (14).

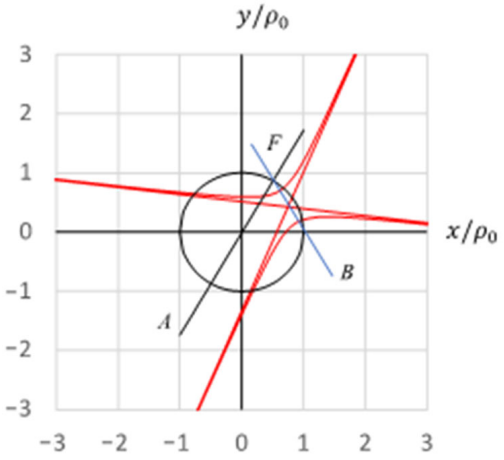

(**a**)

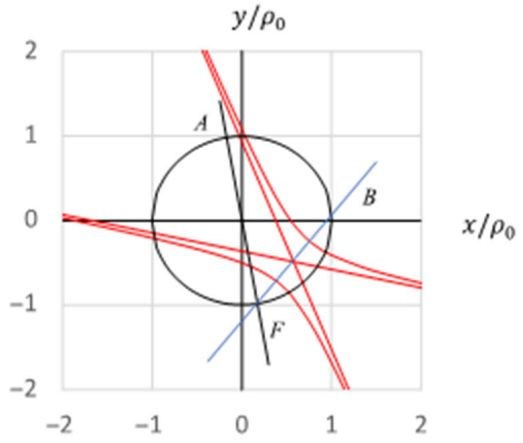

(**b**)

Figure 2. Examples of the dependence of the normalized ordinate $y/\rho_0=(\rho/\rho_0)\sin\phi$ on the normalized abscissa $x/\rho_0=(\rho/\rho_0)\cos\phi$; $\phi_2=60°$ (**a**), $\phi_2=-80°$ (**b**); AF—line passing through the origin, on which focus F is located, B—its symmetric second focus.

This choice of coordinate system eliminates the need for strict synchronization of the motion of the UAVs forming the group. A circle can always be defined through any three non-collinear points; therefore, the adopted coordinate framework is preserved for any mutual arrangement of the UAVs.

Figure 3 shows an example of the dependence of the parameter s on the angle ϕ. As expected, the parameter s tends to infinity as the angle ϕ approaches the value determined by the equation

$$\sin^2\frac{\varphi_2}{2}\sin^2\left(\varphi-\frac{\varphi_2}{2}\right)-q^2=0 \tag{18}$$

These values correspond to the asymptotes of the resulting hyperbola.

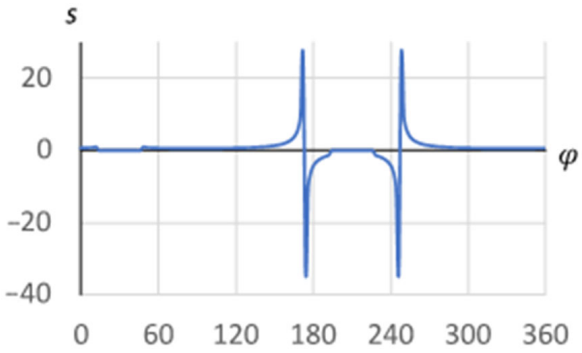

Figure 3. Example of the dependence of the parameter s on the angle ϕ; $\phi_2 = 60^\circ$.

This example shows that large values $s \gtrsim 8$ occur only when φ approaches the angle defined by Equation (18). This implies that, for solving the localization problem, it is reasonable to exploit the asymptotic behavior of the hyperbolas, since the signal source is assumed to be located at a distance much larger than ρ_0 from the origin.

This conclusion is illustrated in Figure 4, which shows an example of the intersection of two hyperbolas generated by two phase differences recorded by two UAV pairs.

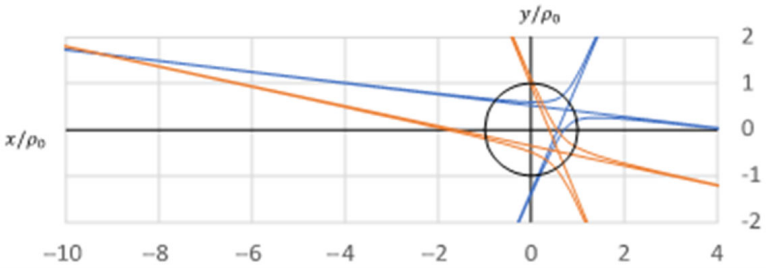

Figure 4. Illustration of the determination of the intersection points of the hyperbolas.

This example qualitatively demonstrates the following preliminary conclusion, which ensures the uniqueness of the solution to the problem under consideration. Specifically, from the standpoint of determining the coordinates of the signal source, only the intersection point lying outside the circle used to construct the chosen coordinate system is of practical interest. To justify this conclusion quantitatively, we use the equation

$$\left(r_1^2-r_2^2\right)^2-2R^2\left(r_1^2+r_2^2\right)+R^4=0 \tag{19}$$

where $r_{1,2}^2 = (\vec{r}-\vec{r}_{10,20})^2$.

The same preliminary conclusion is also supported by the results of computer experiments (the code used is provided in the Supplementary Materials). Figure 5 presents plots showing the hyperbola asymptotes and their intersection points under specific model conditions. It can be seen that the proposed method indeed makes it possible to determine

the operator's coordinates with an accuracy acceptable for the intended purposes, and that the accuracy increases as the ratio $\frac{D}{R}$ grows, where D is the distance from the center of the circle on which the UAVs are located to the operator.

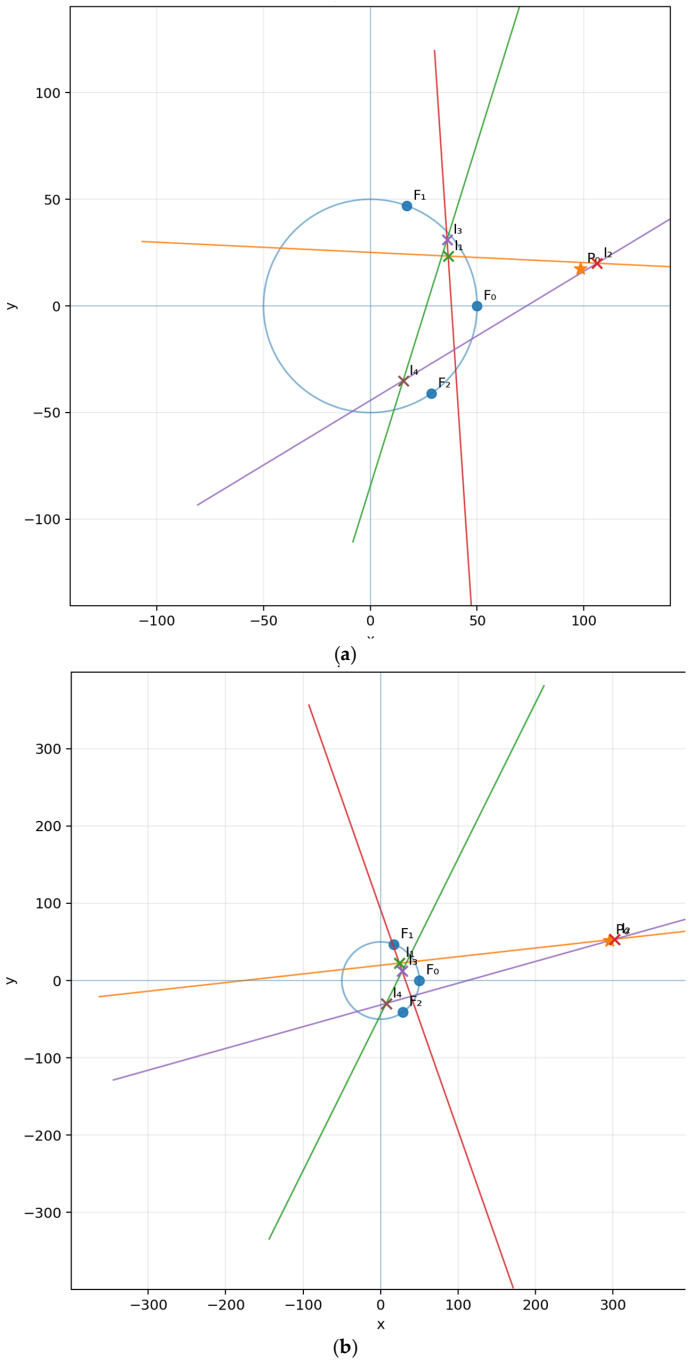

Figure 5. Location of the hyperbola intersection points under the specified model conditions: **(a)** R = 50, $\varphi_1 = 70°$, $\varphi_2 = -55°$, $\rho_0 = 100$, $\theta_0 = 10°$, **(b)**—$R = 50$, $\varphi_1 = 70°$, $\varphi_2 = -55°$, $\rho_0 = 300$, $\theta_0 = 10°$ (based on the results of a computer experiment). Circular arc/curve: the circle of radius R, on which the hyperbola foci are placed. Filled circles (•): the foci of the two hyperbolas: F_0 (the common focus on the x-axis), and the two non-common foci F_1 and F_2 determined by the angles φ_1 and φ_2. Star marker (★): the reference point P_0 given in polar coordinates (ρ_0, θ_0). This point is used to define the hyperbola parameters (via Δ_1 and Δ_2, unless stated otherwise). Straight lines (two per hyperbola): the asymptotes of each hyperbola. Each hyperbola contributes two asymptote lines. Cross markers (×): the intersection points of the asymptotes, denoted I_1, I_2, I_3, I_4. These are the four points of interest produced by pairwise intersections of the two asymptote pairs.

Equation (19) follows directly from Equation (5) and can be obtained by squaring it twice, taking into account the specifics of the adopted coordinate system, in which all UAV positions lie on a single circle. We now derive the asymptotic solution of Equation (19) corresponding to a straight line. We seek this solution in the parametric form

$$\vec{r} = t\vec{e} + \frac{1}{2}\left(\vec{r}_{01} + \vec{r}_{02}\right) \tag{20}$$

where $\vec{r}$ is the current radius vector, t is a scalar parameter, and $\vec{e}$ is a unit vector defining the direction of the straight line,

$$\vec{e} = (\cos\alpha, \sin\alpha) \tag{21}$$

The constant term in Equation (20) is chosen for evident geometric reasons: the asymptote of a hyperbola generated by a particular UAV pair must pass through the midpoint of the segment connecting their locations. Substituting Equation (20) into Equation (19), and using the fact that in the adopted coordinate system $r_{10}^2 = r_{20}^2$, we obtain after straightforward transformations:

$$4t^2\left(\left(\vec{r}_{10} - \vec{r}_{20}\right)\vec{e}\right)^2 - 4R^2t^2 + const = 0 \tag{22}$$

Since we are seeking the asymptote, it is permissible to equate to zero the coefficient of t^2. Note also that the absence of a linear term in t confirms the correctness of the choice of the parametric form (20). Thus, Equation (22) effectively reduces to an equation for the direction of the unit vector $\vec{e}$. Indeed, in the asymptotic limit Equation (22) becomes

$$\left(\left(\vec{r}_{10} - \vec{r}_{20}\right)\vec{e}\right)^2 = R^2 \tag{23}$$

Furthermore,

$$\left(\vec{r}_{10} - \vec{r}_{20}\right)\vec{e} = 2\rho_0 sin\frac{\varphi_2 - \varphi_1}{2} sin\left(\varphi - \frac{\varphi_2 + \varphi_1}{2}\right) \tag{24}$$

which yields the expression for the angle α defining the direction of the hyperbola asymptotes in the chosen coordinate system:

$$\sin^2\left(\alpha - \frac{\varphi_2 + \varphi_1}{2}\right) = \frac{R^2}{4\rho_0^2 \sin^2\frac{\varphi_2 - \varphi_1}{2}} \tag{25}$$

This result agrees with Equation (18), given that $q = R/(2\rho_0)$.

The derived relation makes it possible to address the question of the uniqueness of determining the coordinates of the signal source. As follows from the considerations illustrated in Figures 3 and 4, when the source is sufficiently far from the circle used to construct the coordinate system, the intersections of the hyperbola asymptotes—i.e., the four straight lines—may be used instead. Excluding the intersections of asymptotes belonging to the same hyperbola, the total number of intersection points is four. One must then select the point that is physically relevant for the problem at hand. We now show that, in general, this selection can indeed be made in a manner consistent with practical applications.

We specify the asymptotes in parametric form as

$$\vec{r}_i = l_i\vec{e}_i + \vec{r}_{0i},\ i = 1, 2, 3, 4 \tag{26}$$

where $\vec{e}_i = (\cos\alpha_i, \sin\alpha_i)$ is the unit vector defining the direction of the i-th asymptote, determined from Equation (24), and $\vec{r}_{0i}$ is the radius vector of the midpoint of the segment connecting the corresponding UAV pair. The parameter l_i has the dimension of length, and the index i enumerates the four lines shown in Figure 6.

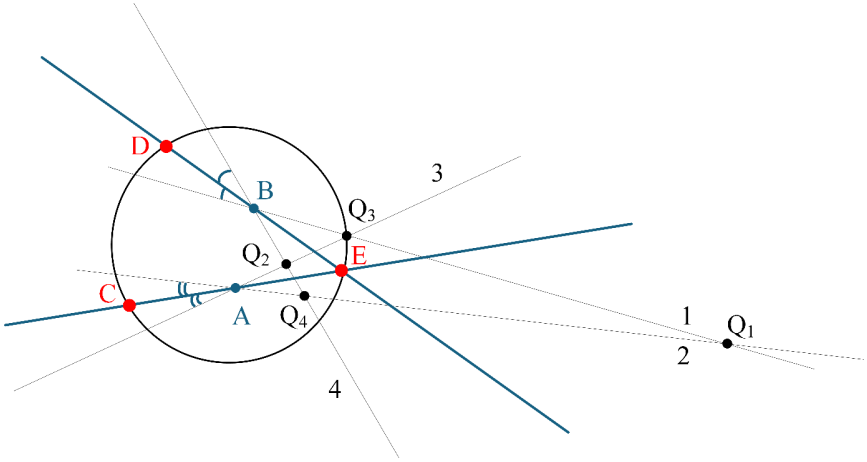

Figure 6. On the issue of the uniqueness of determining the coordinates of the signal source using the method of intersecting hyperbola asymptotes; C, D, E denote the UAV positions.

The intersection point of two straight lines (lines 1 and 2 in Figure 5) is obtained from the equations

$$0 = l_1\cos\alpha_1 - l_2\cos\alpha_2 + x_{10} - x_{20} \tag{27}$$

$$0 = l_1\sin\alpha_1 - l_2\sin\alpha_2 + y_{10} - y_{20} \tag{28}$$

where $l_{1,2}$ are the distances from the intersection point to the reference points at which $l_{1,2} = 0$. Combining Equations (27) and (28) in a standard way yields

$$l_1 = \frac{(x_1 - x_2)\sin\alpha_2 - (y_1 - y_2)\cos\alpha_2}{\sin(\alpha_1 - \alpha_2)} \tag{29}$$

The vector

$$\vec{e}_{2\perp} = (\sin\alpha_2, -\cos\alpha_2) \tag{30}$$

is orthogonal to the vector $\vec{e}_2 = (\cos\alpha_2, \sin\alpha_2)$, which defines the direction of the corresponding asymptote:

$$\vec{e}_{2\perp}\vec{e}_2 = \sin\alpha_2\cos\alpha_2 - \cos\alpha_2\sin\alpha_2 = 0 \tag{31}$$

Therefore, expression (29) can be rewritten as

$$l_1 = \frac{\left(\vec{r}_{01} - \vec{r}_{02}\right)\vec{e}_{2\perp}}{\sin(\alpha_1 - \alpha_2)} \tag{32}$$

Similarly,

$$l_2 = \frac{\left(\vec{r}_{01} - \vec{r}_{02}\right)\vec{e}_{1\perp}}{\sin(\alpha_2 - \alpha_1)} \tag{33}$$

For the numerators in Equations (32) and (33), the following inequality holds:

$$0 \le \left(\vec{r}_{01} - \vec{r}_{02}\right)\vec{e}_{2\perp} \le \Delta l_{12} \tag{34}$$

where Δl_{12} is the distance between UAVs 1 and 2.

In particular, this implies that when the location of a signal source sufficiently far from the circle used as the reference frame is determined (i.e., $l_i \gg \rho_0$), the following relation must hold:

$$\alpha_2 \approx \alpha_1 \tag{35}$$

This approximate equality means that the directions of the hyperbola asymptotes associated with two different UAV pairs must nearly coincide. In Figure 6, these are lines 1 and 2, which intersect at point Q_1.

Each hyperbola also has a second asymptote, shown as lines 3 and 4. Accordingly, there exist three additional intersection points of asymptotes belonging to different hyperbolas, labeled Q_2–Q_4.

From inequalities (32) and (33), the following estimate is valid for these points:

$$0 \le l_i \le \frac{\Delta l_{i,j}^2}{R} \tag{36}$$

Similar considerations apply to point Q_2.

The obtained result resolves the issue of uniqueness when locating a radio signal source positioned more than approximately $5\rho_0$ away from the UAV group. Specifically, all points except Q_1 lie at distances on the order of ρ_0 from the origin, which is also clearly illustrated in Figure 4. Therefore, to solve the problem, it is sufficient to compute the distances to all four asymptote intersection points and select the largest one.

This conclusion is illustrated by the results of the numerical experiment presented in Table 1. It can be seen that, as follows from the considerations discussed above, the proposed method enables the operator's coordinates to be determined with acceptable accuracy under the condition $D \gg R$; specifically, the present experiment indicates that the requirement $D \ge 6R$ should be satisfied. The experiment also shows that the choice of the intersection point should be made according to the criterion stated above: the intersection point farthest from the center of the circle on which the UAVs are located should be selected. This criterion is likewise valid when the condition $D \gg R$ holds.

Table 1. Results of computing the coordinates of the four intersection points of the asymptotes in normalized polar coordinates $\left(\frac{\rho_k}{R},\ \psi_k\right)$, where ψ_k is given in degrees, R is the radius of the circle on which the UAVs are located, and k is the index of the intersection point (ordered by distance). The computations are reported for the specified parameter sets $(\varphi_1, \varphi_2, D/R, \theta)$, where φ_1 and φ_2 are the angles defining the UAV positions, and $\left(\frac{D}{R},\ \theta\right)$ are the normalized true polar coordinates of the signal source.

Case	φ_1, °	φ_2, °	D	θ, °	k	ρ_k/R	ψ_k, °
Case 1	40	220	5	60	3	6.895	−111.332
					4	6.410	−111.374
					2	5.019	60.016
					1	4.667	59.958
Case 2	60	200	6	300	3	6.314	−59.706
					1	1.331	−53.312
					2	0.893	−136.481
					4	0.788	−134.831
Case 3	30	210	10	135	3	9.870	135.040
					2	7.292	−16.721
					1	1.648	−39.963
					4	1.283	169.748

The obtained results show that the signal source coordinates can be determined with acceptable accuracy using extremely simple algorithms that reduce the problem to

computing the intersection points of straight lines, where the parameters of these lines are also calculated using relatively simple expressions of the form (25). The relatively low accuracy in determining the signal source coordinates is due to, the nature of the tasks for which the proposed method was developed. One of these tasks is the identification of a signal source according to the "friend–foe" principle, performed by a group of UAVs operating in close proximity to the line of contact. In this case, the regions where signal sources generated by the opposing side are certainly absent are defined in advance. Moreover, provided that the line of contact is well-defined, it is sufficient for the above identification to establish the direction to the signal source; thus, errors in estimating the range to the signal source become even less significant.

The proposed mathematical framework enables the use of the simplest possible algorithms that support "friend–foe" identification of a signal source, which is important also from the standpoint of reducing the computational load on onboard systems.

The nature of the tasks addressed is also related to the fact that the use of UAVs (including combat applications) is becoming increasingly widespread, and economic factors are playing an ever more important role (reducing the cost of UAVs and their groups). In particular, UAVs are being deployed on an increasingly large scale in the vicinity of the line of contact. This, in turn, implies that a significant portion of the electronic warfare (EW) assets employed by the opposing sides is also located close to the line of contact. Consequently, the sources of signals intended to counteract systems of the type considered here are, with high probability, likewise situated within line-of-sight radio visibility. Such signals can nevertheless degrade the system's performance. More precisely, under external informational interference, the method we propose allows only the identification of the very fact of such interference. In our view (based, among other things, on an analysis of UAV employment in the ongoing conflict in Ukraine), this apparent limitation can be turned into an advantage. Detecting the location of an external signal source is often a far more important task than suppressing it.

Indeed, there is little doubt that, as the cost of UAVs (and their groups) continues to decline, countermeasures should focus on identifying the operators' deployment locations. Therefore, when "friend–foe" identification of the command signal is not feasible, it is reasonable to employ an algorithm in which the UAV group transmits to the operator a signal instructing them to switch to radio silence. The group then transitions to a mode for localizing the external signal source (potentially also adapting the nature of the mission in light of the economic considerations noted above).

The results of the computer experiments are presented in greater detail in Figures 6–8. Figure 6 shows an example outcome of a computer experiment, namely the dependence of ΔD (the deviation of the estimated distance to the signal source from its true value) on the parameter D, which is the distance from the signal source to the center of the circle on which the UAVs are located. It can be seen that this deviation decreases rather sharply as D increases.

Figure 7 provides another example result of a computer experiment: the dependence of $\Delta\psi = \psi - \psi_0$ (ψ is the estimated bearing angle to the signal source, and ψ_0 is the true angle) on D. This result also corroborates the conclusion stated above: the accuracy of estimating the operator's coordinates improves as the ratio D/R increases.

Figure 8 summarizes the results of a computer experiment designed to assess how errors in measuring the differences of time of arrival affect the accuracy of determining the operator's coordinates. The figure shows the intersection points of the hyperbola asymptotes, one of which corresponds to the estimated operator position, as well as the point corresponding to the true position. In the experiment, a controlled error of 3% and 5% was artificially introduced into the values $c\Delta t_{12}$ and $c\Delta t_{23}$ for the considered model

example. It can be seen that, in this case as well, the accuracy of operator localization remains adequate for the stated objective (identifying the signal source using a "friend-or-foe" principle, under the assumption that a region has been specified where sources belonging to the opposing side cannot be located).

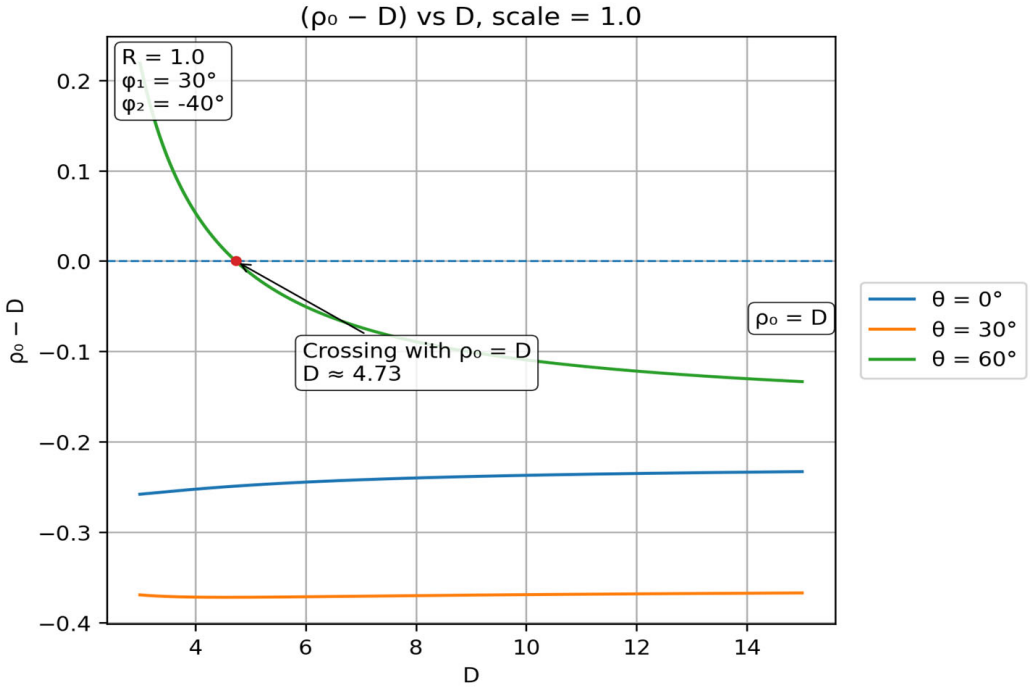

Figure 7. Dependence of ΔD (the deviation of the estimated distance to the signal source from the true value of this parameter) on D.

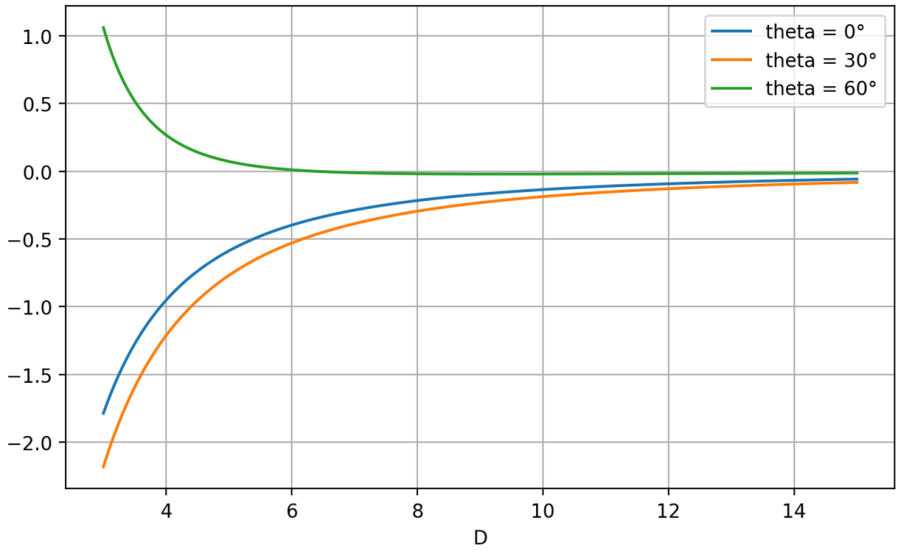

Figure 8. Dependence of the deviation of the estimated bearing angle (direction to the signal source) from the true value on the parameter D; three values of the source bearing angle were used (indicated in the figure). The y-axis shows $\Delta\psi$, and the x-axis shows D.

The computer experiments also revealed that degenerate cases may occur (Figure 9), in which the hyperbola asymptotes are nearly parallel and form only a small angle with respect to each other. In such cases, ΔD may reach relatively large values; however, this does not always materially affect the proposed information-protection method. For instance, if a UAV group is deployed in close proximity to the combat engagement area, it may be sufficient to determine not the full coordinates of the signal source but only its directional

(bearing) angle. The case shown in Figure 9 indicates that, under such conditions, the bearing angle can be estimated with acceptable accuracy even for comparatively small values of the parameter D/R.

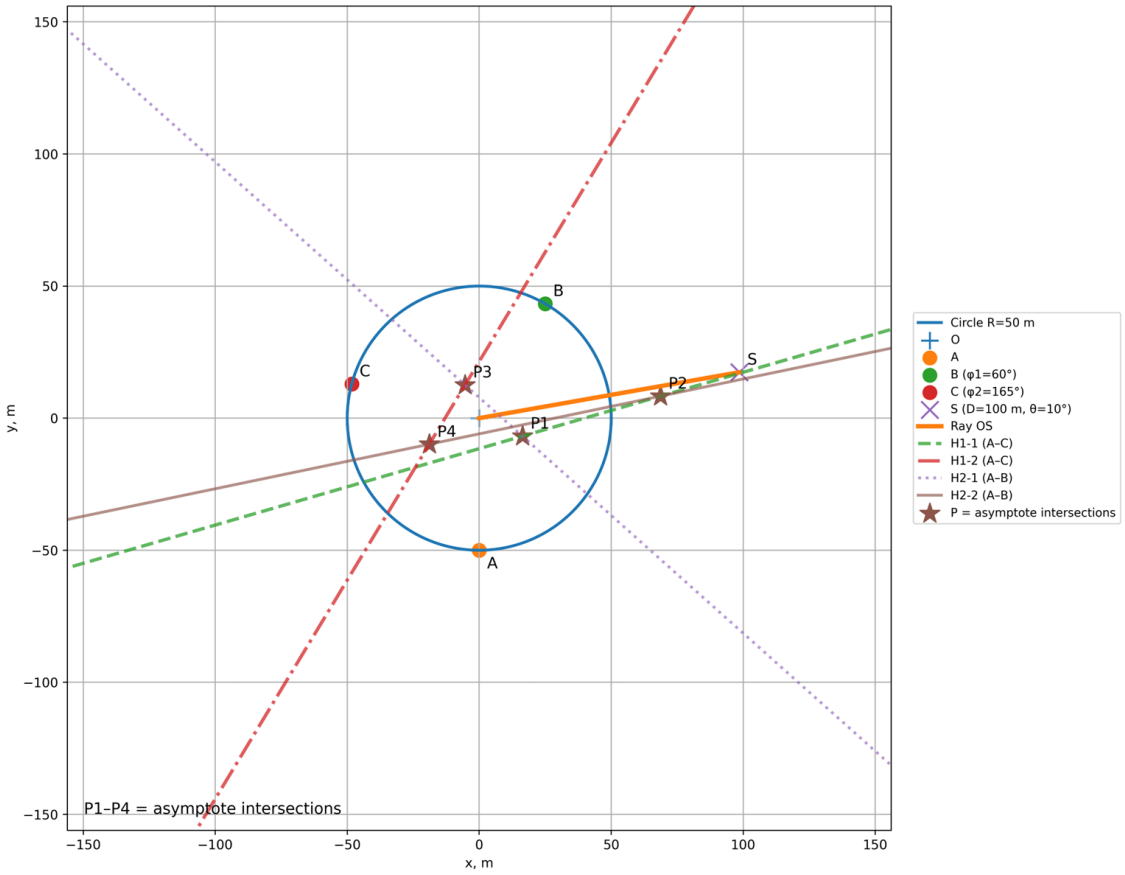

Figure 9. Illustration of the possibility of estimating the bearing angle in a pronounced degenerate case; computer experiment conditions: $R = 50$, $\varphi_1 = 60^\circ$, $\varphi_2 = 165$, $\rho_0 = 100$, $\theta_0 = 10^\circ$, Δ error +5%.

Table 2 presents a comparison of the main characteristics of the proposed method with previously known approaches.

Table 2. Comparison of Key Characteristics of the Proposed Method with Existing Approaches.

Criterion	Proposed method (this paper): 3-UAV formation + intra-group fiber + hyperbola-asymptote intersections	Classical TDoA multilateration (full hyperbola intersection, numerical)	Cryptography-based secure RF control for swarms	Direct long fiber-optic control (operator–UAV tether)	Angle of Arrival/ Direction of Arrival (AoA/DoA) direction-finding (directional/array-based)
Primary goal	Physical protection of command transmission + unambiguous emitter/operator localization	Localization accuracy (position estimation)	Confidentiality/ authentication of commands	Maximal interference immunity for control link	Localization by bearing estimation
Main observable	TDoA/phase-difference between UAV pairs + geometric criterion via asymptotes	TDoA between multiple receivers	Crypto primitives over RF link	Wired optical channel	Angle-of-arrival/bearing
Minimal number of airborne nodes	3 UAVs (two pairs)	Typically $\geq$3 receivers; often more for robustness	Any (depends on network topology)	1 UAV per tethered link	Typically $\geq$2 bearings (or $\geq$1 with motion/array)

Table 2. *Cont.*

Time synchronization requirement	Simplified by fiber SYNC distribution; time resolution error $\leq 10\%$ acceptable in experiments	Requires tight synchronization across receivers; accuracy strongly tied to clocking	Not a localization method; sync depends on wave-form/protocol	Sync not critical for security (wired)	Sync not primary; calibration/phase coherence may be required
Ambiguity handling	Guaranteed disambiguation: pick the asymptote-intersection point farthest from formation center; spurious points remain near formation radius	Multiple intersections may occur; disambiguation often heuristic or via extra constraints/sensors	Does not resolve geometric ambiguity; only secures payload	No ambiguity in channel security; localization not inherent	Bearing intersections can be ambiguous under multipath/geometry
Computation	Light: compute asymptote directions + up to 4 intersections + select max distance	Heavier: solve nonlinear system/intersect hyperbolas numerically	Low/medium (depends on crypto suite)	Low (channel)/high mechanical burden	Medium/high (array processing, calibration)
Resistance to external RF interference	High for intra-group coordination (fiber) + "friend–foe" source attribution for commands under Line-of-sight (LoS)	Potentially vulnerable (RF front-ends + spoofing/jamming)	Vulnerable to jamming even if encrypted; key compromise/ human factor possible	Very high against RF interference, but heavy/complex	Vulnerable to jamming and multipath; depends on SNR/array
Operating conditions emphasized	Line-of-sight (LoS) use case; emitter/operator/EW localization in LoS zone	Broad (LoS/Non-Line-of-Sight (NLoS), but NLoS degrades	Broad	Physical constraints dominate; cable length/weight issues	Works best in LoS; multipath degrades
Swarm-motion synchronization	Not required: coordinate frame defined by circle through 3 UAVs; works for any mutual geometry	Not a swarm sync method; may need stable geometry assumptions	Requires network coordination; swarm synchronization is a separate problem	Not a swarm method per se	Not a swarm sync method
Scalability (adding nodes)	Can expand with additional UAVs using directional antennas and low-power relays (3-UAV core as reference/relay)	Scales by adding receivers but increases sync/processing burden	Scales naturally, but attack surface grows with complexity	Poor (tethers do not scale well)	Scales with additional bearings/arrays but increases HW complexity
Typical trade-off	Reduced algorithmic complexity + physical protection within group; relaxed operator-localization accuracy in some scenarios	Better accuracy possible, but higher requirements for sync and robust disambiguation	Strong for confidential-ity/authentication, weaker against jamming	Strong physical security, strong practical constraints (mass/length)	Good for direction cues; hardware/ calibration burden

5. Discussions

The proposed approach can also be used to determine the coordinates of external radio signal sources (for example, positions of opposing drone operators or electronic warfare (EW) systems). The operating principle remains the same; the only difference lies in the required accuracy of locating the signal source. This method is applicable exclusively within the line-of-sight zone. However, as current experience from the conflict in Ukraine demonstrates, electronic warfare systems deployed near the line of contact are becoming increasingly significant. Consequently, developing technical tools that enable counter-operations is also relevant.

Such tools must be maximally resistant to potential hostile interference—at least in terms of information security. The use of fiber-optic communication lines between UAVs within a group inherently prevents such interference.

The proposed approach, in the long term, also makes it possible to increase the number of UAVs in the group without using fiber-optic communication. The corresponding scheme is shown in Figure 6. The group includes three UAVs (1) connected by fiber-optic lines (2), and an additional UAV (4) equipped with directional antennas (5). Group control

is performed by operator (3) using the method described in [15]. The uniqueness of determining the operator's coordinates has been proven above.

In this configuration, the main group of three UAVs (1) also serves as a relay for the control signal transmitted to UAV (4) (Figure 10). Several such UAVs may be included in the group. In the simplest case, information security against external attacks is ensured by comparing commands received from three independent sources. The use of directional antennas, at minimum, makes it possible to identify adversarial interference based on purely geometric factors. This can be illustrated by UAV deployments in the ongoing conflict in Ukraine: in many cases, the effective width of the contact zone approximately corresponds to the line-of-sight radio range (up to about 2 km). Under such conditions, establishing additional command-transmission channels over the radio link by the opposing side is, at the very least, difficult. Consequently, receiving identical commands from different directions enables attribution of the received command according to a "friend–foe" principle.

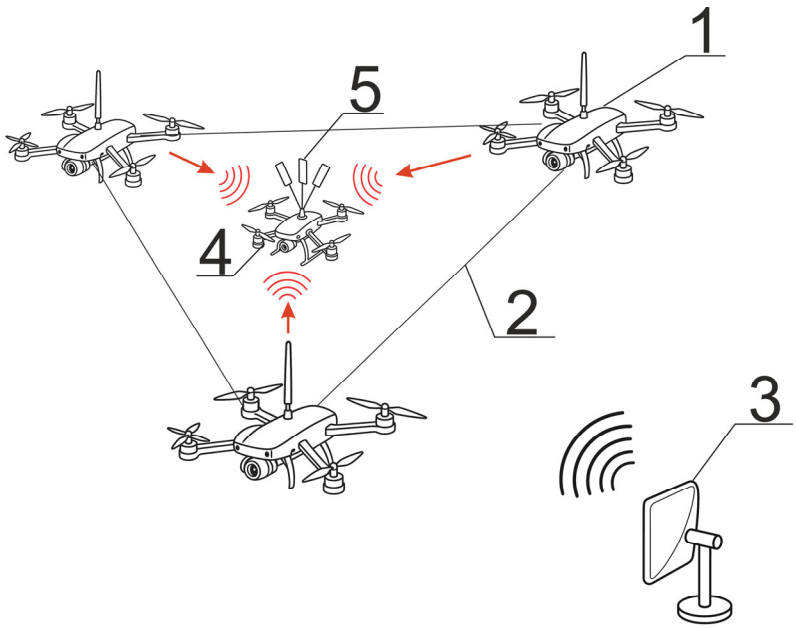

Figure 10. Use of directional antennas to increase the number of UAVs in the group (UAVs (1) fiber-optic lines (2), an additional UAV (4) directional antenna (5), operator (3)).

Estimates of the radiation-pattern characteristics of antennas deployed on additional elements of a UAV group—elements that can be integrated into the group without fiber-optic communication—can be derived from geometric considerations. The beamwidth (aperture angle) of the antenna radiation pattern should be such that any signal received by this element can be unambiguously attributed to only one of the main elements of the group located at the vertices of the triangle. Assuming that the triangle formed by the UAVs is sufficiently close to equilateral (specifically, none of its sides exceeds any other side by more than a factor of two), and that the additional element is located approximately at the intersection point of the medians (within a 10% deviation), the admissible beamwidth varies within the range from 70 to 180 degrees, which is a completely achievable characteristic even for directional antennas of the simplest types.

From a similar standpoint, the required accuracy of estimating the operator's coordinates can also be considered. Any improvement in this capability is associated with increased cost, which is particularly relevant for military applications of robotic systems. At the same time, when a UAV group employs the proposed approach, the accuracy requirements for localizing the operator can be deliberately relaxed. Indeed, in this case it

is sufficient to obtain only an approximate operator position, since the probability that electronic-warfare units would be located within the immediate vicinity of their own forward positions is negligible due to the associated risk. On this basis, one may conclude that the proposed approach remains applicable at the operator-localization error levels observed, including those used in the computer experiments.

For additional protection (in applications other than the above), various lightweight cryptographic protocols may be employed, for example, those analogous to [60–63], as well as data obfuscation techniques [64–66].

This is entirely sufficient, since UAV (4) can be controlled using low-amplitude signals detectable only in the immediate vicinity of the group. Data obfuscation may also be implemented using the method of computing partial discrete logarithms proposed in [67]. This method, which is based on the use of an algebraic delta-function [68], fundamentally differs from known discrete logarithm algorithms [69–72]: it yields explicit algebraic formulas and significantly reduces the number of required operations [67].

Importantly, element (4) in the group may also be a ground-based drone. Clearly, controlling such drones via optical fiber is technically infeasible due to obstacles such as trees and terrain irregularities. Consequently, the deployment of ground drones is inherently constrained by electronic warfare factors. The proposed scheme removes these limitations. This example further highlights the relevance of developing information-protection systems under line-of-sight conditions: ground drones are inherently intended for operation primarily near the line of contact. Developing specific control schemes for ground drones will, of course, require further research; however, this example already indicates that the proposed approach has substantial potential for continued development. Below, we provide another example illustrating this conclusion.

We emphasize that the example presented below is purely illustrative; that is, this brief consideration of the system is intended to demonstrate clearly that, in the future, a group of the proposed type may also include additional UAVs, where these additional UAVs are not connected to the main fiber-optic links. (Here, the term “main UAVs” refers to the vehicles that provide information protection in accordance with the proposed method.)

This approach also addresses several operational challenges observed during the current military conflict in Ukraine. In particular, combat use of drones is typically limited to relatively short ranges (e.g., attacks on heavy military equipment). This makes drones detectable and allows effective countermeasures. The group schematically depicted in Figure 6 may be equipped with components designed to mitigate this limitation. As an illustration, consider the design proposed in [73]. Its prototype is the configuration introduced in [74], which combines the advantages of propeller-driven and jet propulsion (Figure 11).

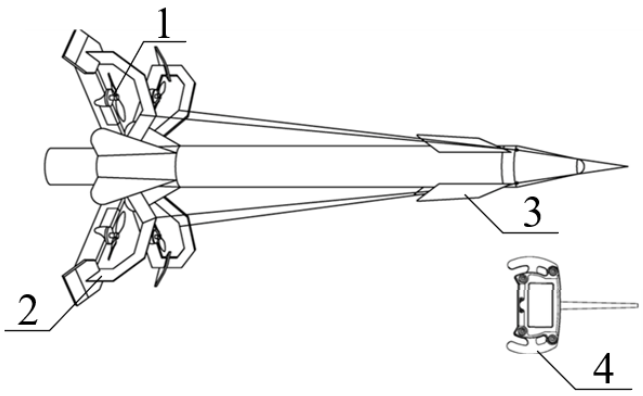

Figure 11. Example of a system combining propeller-driven and jet thrust: 1—propeller, 2—wings, 3—wings of the auxiliary rocket, 4—wireless control unit.

In the long term, such designs are capable of fulfilling the same function currently performed by guidance kits mounted, for example, on general-purpose aerial bombs. An unguided bomb trajectory makes the carrier aircraft vulnerable to enemy air-defense systems, whereas the ability to correct the trajectory significantly reduces this vulnerability.

Similarly, the combination of propeller-driven and jet thrust allows the trajectory of an unmanned aerial vehicle to be divided into two segments. Movement along the first segment is performed using propeller-driven thrust, while the second segment (which includes target acquisition and the final high-speed approach) is performed using jet propulsion.

The design presented in [73] and shown in Figure 12 performs an analogous function, but it is optimized specifically for jet propulsion based on the laws of classical mechanics.

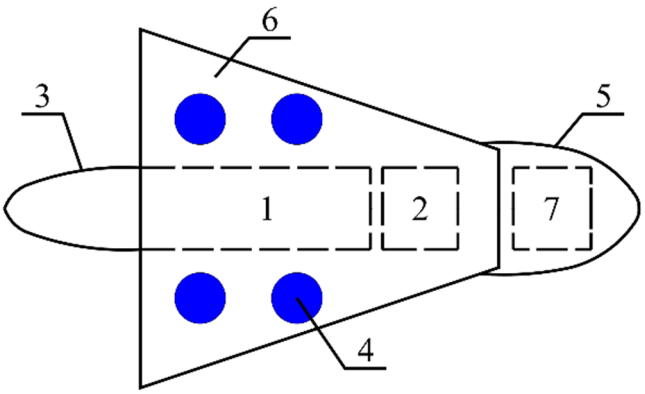

Figure 12. Diagram of a kamikaze drone with jet-assisted targeting of the warhead.

The proposed configuration includes the following components:
1—warhead;
2—charge equipped with a detonator;
3—warhead fairing;
4—propeller motors similar to those currently used in quadcopters;
5—fairing of the main body;
6—main body equipped with stabilizers;
7—remote control unit.

The core of this design is the main body, consisting of components (5) and (6). It carries the propeller motors (4), which ensure its movement through the air in the same manner as a quadcopter. Inside the body are located the warhead (1) with its fairing (3), the detonator-equipped charge (2), and the control unit (7).

When approaching the target to the required engagement distance, the system is aimed at the target by adjusting its orientation using the propeller motors (4). The detonator in charge (2) is then activated, imparting non-zero impulses to both the warhead and the main body in opposite directions. The warhead is directed toward the target, while the main body is propelled in the reverse direction. The stability of the initial velocity vector of the warhead is ensured by the stabilizers on the main body (6). In a sense, the main body acts as an analog of a jet-propelled device whose motion in a given direction is ensured by stabilizers and by the separation of the warhead. This ensures warhead targeting directly following the vector form of the conservation of momentum:

$$m_1 \vec{v}_1 = m_2 \vec{v}_2 \tag{37}$$

where m_1 is the mass of the warhead (including its carrier), m_2 is the mass of the material providing the jet propulsion (i.e., the mass of the main body), $\vec{v}_2$ is its velocity vector, and $\vec{v}_1$ is the velocity vector of the warhead.

For the considered configuration, one may formulate the following problem: what should be the ratio of m_1 to m_2 in order to maximize the destructive effect (determined by the warhead's momentum)? Taking into account the conservation of energy, it is straightforward to show that the masses of the warhead and the main body should be equal.

Several additional examples could be given to demonstrate that the scheme shown in Figure 6 indeed enables the deployment of a wide range of UAV group configurations for various operational purposes.

6. Conclusions and Future Work

A novel geometric method for unambiguous localization of remote radio-signal sources using three UAVs connected by fiber-optic links, relying on the intersection of hyperbola asymptotes rather than full hyperbola curves, is presented. We show that the physically correct emitter location is always the asymptote-intersection point farthest from the UAV formation center, while all spurious solutions remain confined near the formation radius.

The method enables secure, interference-resistant command transmission from the operator to the UAV group and supports the detection of external radio emitters (including operators and electronic-warfare systems) under line-of-sight conditions. Information protection is based on identifying the signal source according to a "friend–foe" principle. The method is particularly effective when the area in which malicious signal sources cannot be located is known in advance at least approximately (for example, on one side or the other of the line of contact). In this case, the operator's coordinates can be estimated with relatively low accuracy, at a level that is attainable for the method under consideration.

The approach provides a scalable foundation for expanding UAV groups with nodes using directional antennas and lightweight protection mechanisms, supporting resilient architectures and advanced configurations such as hybrid-propulsion or jet-assisted UAV platforms.

Supplementary Materials: The following supporting information can be downloaded at https://www.mdpi.com/article/10.3390/drones10010024/s1, S1: Commented Python listing.

Author Contributions: Conceptualization, I.S.; Methodology, I.S.; Investigation, D.S. and A.K.; Resources, D.S.; Data curation, D.S.; Software, Y.V. and A.K.; Validation, Y.V. and A.K.; Formal analysis, A.K.; Visualization, Y.V.; Supervision, Y.V.; Project administration, Y.V.; Funding acquisition, Y.V. and I.S.; Writing—original draft preparation, I.S.; Writing—review and editing, D.S., A.K. and Y.V. All authors have read and agreed to the published version of the manuscript.

Funding: This research is funded by the Science Committee of the Ministry of Science and Higher Education of the Republic of Kazakhstan (BR24992908 "Support system for agricultural crop production optimization via remote monitoring and artificial intelligence methods (Agroscope)").

Data Availability Statement: The original contributions presented in this study are included in the article and Supplementary Materials.

Conflicts of Interest: The authors declare no conflicts of interest.

References

1. Abdelkader, M.; Güler, S.; Jaleel, H.; Shamma, J.S. Applications and challenges. *Curr. Robot. Rep.* **2021**, *2*, 309–320. [CrossRef] [PubMed]
2. Wang, C.; Su, Y.; Wang, J.; Wang, T.; Gao, Q. UAV swarm dataset: An unmanned aerial vehicle swarm dataset for multiple object tracking. *Remote Sens.* **2022**, *14*, 2601. [CrossRef]
3. Mukhamediev, R.I.; Yakunin, K.; Aubakirov, M.; Assanov, I.; Kuchin, Y.; Symagulov, A.; Levashenko, V.; Zaitseva, E.; Sokolov, D.; Amirgaliyev, Y. Coverage Path Planning Optimization of Heterogeneous UAVs Group for Precision Agriculture. *IEEE Access* **2023**, *11*, 5789–5803. [CrossRef]

4. Ming, R.; Jiang, R.; Luo, H.; Lai, T.; Guo, E.; Zhou, Z. Comparative analysis of different UAV swarm control methods on unmanned farms. *Agronomy* **2023**, *13*, 2499. [CrossRef]
5. Ali, Z.A.; Deng, D.; Shaikh, M.K.; Hasan, R.; Khan, M.A. AI-Based UAV Swarms for Monitoring and Disease Identification of Brassica Plants Using Machine Learning: A Review. *Comput. Syst. Sci. Eng.* **2024**, *48*, 1–34. [CrossRef]
6. Alqefari, S.; Menai, M.E.B. Multi-UAV task assignment in dynamic environments: Current trends and future directions. *Drones* **2025**, *9*, 75. [CrossRef]
7. Lee, W. Federated reinforcement learning-based UAV swarm system for aerial remote sensing. *Wirel. Commun. Mob. Comput.* **2022**, *2022*, 4327380. [CrossRef]
8. Hu, T.; Zong, Y.; Lu, N.; Jiang, B. Dynamic recovery and a resilience metric for UAV swarms under attack. *Drones* **2025**, *9*, 589. [CrossRef]
9. Ju, C.; Son, H.I. A distributed swarm control for an agricultural multiple unmanned aerial vehicle system. *Proc. Inst. Mech. Eng. Part I J. Syst. Control Eng.* **2019**, *233*, 1298–1308. [CrossRef]
10. Liu, J.; Liao, X.; Ye, H.; Yue, H.; Wang, Y.; Tan, X.; Wang, D. UAV swarm scheduling method for remote sensing observations during emergency scenarios. *Remote Sens.* **2022**, *14*, 1406. [CrossRef]
11. Campion, M.; Ranganathan, P.; Faruque, S. UAV swarm communication and control architectures: A review. *J. Unmanned Veh. Syst.* **2019**, *7*, 93–106. [CrossRef]
12. Gargalakos, M. The role of unmanned aerial vehicles in military communications: Application scenarios, current trends, and beyond. *J. Def. Model. Simul.* **2024**, *21*, 313–321. [CrossRef]
13. Zieliński, T. Factors determining a drone swarm employment in military operations. *Saf. Def.* **2021**, *7*, 59–71.
14. Fedorovych, O.; Kritskiy, D.; Malieiev, L.; Rybka, K.; Rybka, A. Military logistics planning models for enemy targets attack by a swarm of combat drones. *Radioelectron. Comput. Syst.* **2024**, *1*, 207–216. [CrossRef]
15. Suleimenov, I.; Kadyrzhan, A.; Vitulyova, Y.; Shaltykova, D. The use of fiber optics for securing information during command transmission to UAV groups. *Int. J. Inf. Technol.* **2025**. [CrossRef]
16. Lee, J.S.; Yoo, Y.S.; Choi, H.; Kim, T.; Choi, J.K. Group connectivity-based UAV positioning and data slot allocation for tactical MANET. *IEEE Access* **2020**, *8*, 220570–220584. [CrossRef]
17. Hambling, D. Israel Used World's First AI-Guided Combat Drone Swarm in Gaza Attacks. *New Scientist*, 30 June 2021. Available online: https://www.newscientist.com/article/2282656-israel-used-worlds-first-ai-guided-combat-drone-swarm-in-gaza-attacks/ (accessed on 25 December 2025).
18. Alqudsi, Y.; Makaraci, M. UAV swarms: Research, challenges, and future directions. *J. Eng. Appl. Sci.* **2025**, *72*, 12. [CrossRef]
19. Puente-Castro, A.; Rivero, D.; Pazos, A.; Fernandez-Blanco, E. A review of artificial intelligence applied to path planning in UAV swarms. *Neural Comput. Appl.* **2022**, *34*, 153–170. [CrossRef]
20. Rashid, A.B.; Kausik, A.K.; Al Hassan Sunny, A.; Bappy, M.H. Artificial intelligence in the military: An overview of the capabilities, applications, and challenges. *Int. J. Intell. Syst.* **2023**, *1*, 8676366. [CrossRef]
21. McCune, R.; Purta, R.; Dobski, M.; Jaworski, A.; Madey, G.; Madey, A.; Wei, Y.; Blake, M.B. Investigations of DDDAS for command and control of UAV swarms with agent-based modeling. In Proceedings of the 2013 Winter Simulations Conference (WSC), Washington, DC, USA, 8–11 December 2013; pp. 1467–1478. [CrossRef]
22. De La Torre Martín, J. Improving the Robustness of Drone Swarm Control Systems with Graph Learning. Ph.D. Thesis, University of California, Irvine, CA, USA, 2023. Available online: https://escholarship.org/uc/item/5g2676p2 (accessed on 24 November 2025).
23. Guo, C.; Zhu, P.; Zhou, Z.; Lang, L.; Zeng, Z.; Lu, H. Imitation Learning with Graph Neural Networks for Improving Swarm Robustness under Restricted Communications. *Appl. Sci.* **2021**, *11*, 9055. [CrossRef]
24. Chen, L.; Zhu, Y.; Liu, S.; Yu, H.; Zhang, B. PUF-based dynamic secret-key strategy with hierarchical blockchain for UAV swarm authentication. *Comput. Commun.* **2024**, *218*, 31–43. [CrossRef]
25. Dong, R.; Wang, B.; Cao, K. Security enhancement of UAV swarm enabled relaying systems with joint beamforming and resource allocation. *China Commun.* **2021**, *18*, 71–87. [CrossRef]
26. Wang, X.; Zhao, Z.; Yi, L.; Ning, Z.; Guo, L.; Yu, F.R.; Guo, S. A survey on security of UAV swarm networks: Attacks and countermeasures. *ACM Comput. Surv.* **2024**, *57*, 74. [CrossRef]
27. Shen, D.; Chen, X.; Qi, W.; Meng, L. Task allocation for UAV swarms under communication attacks: An approach based on game theory and negotiation mechanism. *J. Frankl. Inst.* **2025**, *362*, 107417. [CrossRef]
28. Jangsher, S.; Al-Dweik, A.; Iraqi, Y.; Pandey, A.; Giacalone, J.P. Group secret key generation using physical layer security for UAV swarm communications. *IEEE Trans. Aerosp. Electron. Syst.* **2023**, *59*, 8550–8564. [CrossRef]
29. Raja, G.; Anbalagan, S.; Ganapathisubramaniyan, A.; Selvakumar, M.S.; Bashir, A.K.; Mumtaz, S. Efficient and secured swarm pattern multi-UAV communication. *IEEE Trans. Veh. Technol.* **2021**, *70*, 7050–7058. [CrossRef]
30. Mohsan, S.A.H.; Othman, N.Q.H.; Li, Y.; Alsharif, M.H.; Khan, M.A. Unmanned aerial vehicles (UAVs): Practical aspects, applications, open challenges, security issues, and future trends. *Intell. Serv. Robot.* **2023**, *16*, 109–137. [CrossRef] [PubMed]

31. Xia, B.; Mantegh, I.; Xie, W. Decentralized UAV Swarm Control: A Multi-Layered Architecture for Integrated Flight Mode Management and Dynamic Target Interception. *Drones* **2024**, *8*, 350. [CrossRef]
32. Sharma, A.; Shoval, S.; Sharma, A.; Pandey, J.K. Path planning for multiple targets interception by the swarm of UAVs based on swarm intelligence algorithms: A review. *IETE Tech. Rev.* **2022**, *39*, 675–697. [CrossRef]
33. Javed, S.; Hassan, A.; Ahmad, R.; Ahmed, W.; Ahmed, R.; Saadat, A.; Guizani, M. State-of-the-art and future research challenges in UAV swarms. *IEEE Internet Things J.* **2024**, *11*, 19023–19045. [CrossRef]
34. Oxford Analytica. Russia's production and use of aerial drones will rise. *Expert Brief.* **2025**. [CrossRef]
35. Martin, G. Are FPV drones the new Precision Guided Munitions? *Asia-Pac. Def. Rep.* **2024**, *50*, 22–25. Available online: https://search.informit.org/doi/abs/10.3316/informit.T202406200000120044433483 5 (accessed on 25 December 2025).
36. Wang, D.; Bai, B.; Zhao, W.; Han, Z. A survey of optimization approaches for wireless physical layer security. *IEEE Commun. Surv. Tutor.* **2018**, *21*, 1878–1911. [CrossRef]
37. Zoli, M.; Mitev, M.; Barreto, A.N.; Fettweis, G. Estimation of the secret key rate in wideband wireless physical-layer-security. In Proceedings of the 2021 International Symposium on Wireless Communication Systems (ISWCS), Berlin, Germany, 6–9 September 2021. [CrossRef]
38. Hamamreh, J.M.; Furqan, H.M.; Arslan, H. Classifications and applications of physical layer security techniques for confidentiality: A comprehensive survey. *IEEE Commun. Surv. Tutor.* **2019**, *21*, 1773–1828. [CrossRef]
39. Ermukhambetova, B.; Mun, G.; Kabdushev, S.; Kadyrzhan, A.; Kadyrzhan, K.; Vitulyova, Y.; Suleimenov, I.E. New approaches to the development of information security systems for unmanned vehicles. *Indones. J. Electr. Eng. Comput. Sci.* **2023**, *31*, 810. [CrossRef]
40. Kuptsov, V.; Badenko, V.; Ivanov, S.; Fedotov, A. Method for Remote Determination of Object Coordinates in Space Based on Exact Analytical Solution of Hyperbolic Equations. *Sensors* **2020**, *20*, 5472. [CrossRef] [PubMed]
41. Alemdar, K.; Varshney, D.; Mohanti, S.; Muncuk, U.; Chowdhury, K. RFClock: Timing, Phase and Frequency Synchronization for Distributed Wireless Networks. In Proceedings of the 27th Annual International Conference on Mobile Computing and Networking, New Orleans, LA, USA, 25–29 October 2021; pp. 15–27.
42. Marrero, L.M.; Merlano-Duncan, J.C.; Querol, J.; Kumar, S.; Krivochiza, J.; Sharma, S.K.; Ottersten, B. Architectures and Synchronization Techniques for Distributed Satellite Systems: A Survey. *IEEE Access* **2022**, *10*, 45375–45409. [CrossRef]
43. Merlo, J.M.; Mghabghab, S.R.; Nanzer, J.A. Wireless Picosecond Time Synchronization for Distributed Antenna Arrays. *IEEE Trans. Microw. Theory Tech.* **2022**, *71*, 1720–1731. [CrossRef]
44. Shamaei, K.; Kassas, Z.M. Receiver Design and Time of Arrival Estimation for Opportunistic Localization with 5G Signals. *IEEE Trans. Wirel. Commun.* **2021**, *20*, 4716–4731. [CrossRef]
45. Zhao, W.; Panerati, J.; Schoellig, A.P. Learning-Based Bias Correction for Time Difference of Arrival Ultra-Wideband Localization of Resource-Constrained Mobile Robots. *IEEE Robot. Autom. Lett.* **2021**, *6*, 3639–3646. [CrossRef]
46. Lu, Y.; Ma, H.; Smart, E.; Yu, H. Real-Time Performance-Focused Localization Techniques for Autonomous Vehicle: A Review. *IEEE Trans. Intell. Transp. Syst.* **2021**, *23*, 6082–6100. [CrossRef]
47. Kuutti, S.; Fallah, S.; Katsaros, K.; Dianati, M.; McCullough, F.; Mouzakitis, A. A Survey of the State-of-the-Art Localization Techniques and Their Potentials for Autonomous Vehicle Applications. *IEEE Internet Things J.* **2018**, *5*, 829–846. [CrossRef]
48. Bresson, G.; Alsayed, Z.; Yu, L.; Glaser, S. Simultaneous Localization and Mapping: A Survey of Current Trends in Autonomous Driving. *IEEE Trans. Intell. Veh.* **2017**, *2*, 194–220. [CrossRef]
49. Manamperi, W.; Abhayapala, T.D.; Zhang, J.; Samarasinghe, P.N. Drone Audition: Sound Source Localization Using On-Board Microphones. *IEEE/ACM Trans. Audio Speech Lang. Process.* **2022**, *30*, 508–519. [CrossRef]
50. Desai, D.; Mehendale, N. A Review on Sound Source Localization Systems. *Arch. Comput. Methods Eng.* **2022**, *29*, 4631–4642. [CrossRef]
51. Yang, T.; Cabani, A.; Chafouk, H. A Survey of Recent Indoor Localization Scenarios and Methodologies. *Sensors* **2021**, *21*, 8086. [CrossRef]
52. Chen, R.; Li, Z.; Ye, F.; Guo, G.; Xu, S.; Qian, L.; Huang, L. Precise Indoor Positioning Based on Acoustic Ranging in Smartphone. *IEEE Trans. Instrum. Meas.* **2021**, *70*, 9509512. [CrossRef]
53. Alsolami, F.; Alqurashi, F.A.; Hasan, M.K.; Saeed, R.A.; Abdel-Khalek, S.; Ishak, A.B. Development of Self-Synchronized Drones' Network Using Cluster-Based Swarm Intelligence Approach. *IEEE Access* **2021**, *9*, 48010–48022. [CrossRef]
54. Pourranjbar, A.; Baniasadi, M.; Abbasfar, A.; Kaddoum, G. A Novel Distributed Algorithm for Phase Synchronization in Unmanned Aerial Vehicles. *IEEE Commun. Lett.* **2020**, *24*, 2260–2264. [CrossRef]
55. Han, S.; Jang, B.-J. Drone's Angle-of-Arrival Estimation Using a Switched-Beam Antenna and Single-Channel Receiver. *Sensors* **2025**, *25*, 2376. [CrossRef]
56. Lutakamale, A.S.; Myburgh, H.C.; de Freitas, A. RSSI-Based Fingerprint Localization in LoRaWAN Networks Using CNNs with Squeeze and Excitation Blocks. *Ad Hoc Netw.* **2024**, *159*, 103486. [CrossRef]

57. Li, M.; Chen, S.-L.; Liu, Y.; Guo, Y.J. Wide-Angle Beam Scanning Phased Array Antennas: A Review. *IEEE Open J. Antennas Propag.* **2023**, *4*, 695–712. [CrossRef]
58. Chen, B.; Ma, J.; Zhang, L.; Zhou, J.; Fan, J.; Lan, H. Research Progress of Wireless Positioning Methods Based on RSSI. *Electronics* **2024**, *13*, 360. [CrossRef]
59. Kadyrzhan, A.; Matrassulova, D.; Vitulyova, Y.; Suleimenov, I. Discrete Cartesian Coordinate Transformations: Using Algebraic Extension Methods. *Appl. Sci.* **2025**, *15*, 1464. [CrossRef]
60. Thakor, V.A.; Razzaque, M.A.; Khandaker, M.R.A. Lightweight Cryptography for IoT: A State-of-the-Art. *arXiv* **2020**, arXiv:2006.13813. [CrossRef]
61. El Gaabouri, I.; Senhadji, M.; Belkasmi, M. A Survey on Lightweight Cryptography Approach for IoT Devices Security. In Proceedings of the 2022 5th International Conference on Networking, Information Systems and Security (NISS), Bandung, Indonesia, 30–31 March 2022; pp. 1–8. [CrossRef]
62. Mouha, N.; Mennink, B.; Herrewege, A.; Watanabe, D.; Preneel, B.; Verbauwhede, I. Chaskey: An Efficient MAC Algorithm for 32-bit Microcontrollers. In *Lecture Notes in Computer Science*; Springer: Cham, Switzerland, 2014; pp. 306–323. [CrossRef]
63. Sysoyev, A.; Nauruzov, K.; Karati, A.; Abramkina, O.; Vitulyova, Y.; Yeskendirova, D.; Popova, Y.; Abdoldina, F. Lightweight Group Signature Scheme Based on PUF for UAV Communication Security. *Drones* **2025**, *9*, 693. [CrossRef]
64. Enireddy, V.; Somasundaram, K.; Prabhu, M.R.; Babu, D.V. Data obfuscation technique in cloud security. In Proceedings of the 2021 2nd International Conference on Smart Electronics and Communication (ICOSEC), Trichy, India, 7–9 October 2021; IEEE: Piscataway, NJ, USA, 2021; pp. 358–362.
65. Gao, Z.; Huang, Y.; Zheng, L.; Lu, H.; Wu, B.; Zhang, J. Protecting location privacy of users based on trajectory obfuscation in mobile crowdsensing. *IEEE Trans. Ind. Inform.* **2022**, *18*, 6290–6299. [CrossRef]
66. Al-Balasmeh, H.; Singh, M.; Singh, R. Framework of data privacy preservation and location obfuscation in vehicular cloud networks. *Concurr. Comput. Pract. Exp.* **2022**, *34*, e6682. [CrossRef]
67. Shaltykova, D.; Vitulyova, Y.; Kadyrzhan, K.; Suleimenov, I. Application of Partial Discrete Logarithms for Discrete Logarithm Computation. *Computers* **2025**, *14*, 343. [CrossRef]
68. Suleimenov, I.E.; Vitulyova, Y.S.; Kabdushev, S.B.; Bakirov, A.S. Improving the Efficiency of Using Multivalued Logic Tools: Application of Algebraic Rings. *Sci. Rep.* **2023**, *13*, 22021. [CrossRef]
69. Adj, G.; Canales-Martínez, I.; Cruz-Cortés, N.; Menezes, A.; Oliveira, T.; Rivera-Zamarripa, L.; Rodríguez-Henríquez, F. Computing discrete logarithms in cryptographically-interesting characteristic-three finite fields. *Cryptol. ePrint Arch.* **2016**, *12*, 741–759. [CrossRef]
70. Zhang, J.; Yang, Y.; Chen, Y.; Chen, F. A secure cloud storage system based on discrete logarithm problem. In Proceedings of the 2017 IEEE/ACM 25th International Symposium on Quality of Service (IWQoS), Vilanova i la Geltru, Spain, 14–16 June 2017; IEEE: Piscataway, NJ, USA, 2017; pp. 1–10.
71. Granger, R.; Kleinjung, T.; Lenstra, A.; Wesolowski, B.; Zumbrägel, J. Computation of a 30750-bit binary field discrete logarithm. *Math. Comput.* **2021**, *90*, 2997–3022. [CrossRef]
72. Wronski, M.; Dzierzkowski, L. Base of exponent representation matters—More efficient reduction of discrete logarithm problem and elliptic curve discrete logarithm problem to the QUBO problem. *Quantum Inf. Comput.* **2024**, *24*, 541–564. [CrossRef]
73. Mun, G.A.; Baipakbayeva, S.T.; Kabdushev, S.B.; Kadyrzhan, K.N.; Kadyrzhan, A.B.; Vitulyova, E.S.; Suleimenov, I.E. Method for Implementing an Unmanned Aerial Vehicle Carrying Air-Launched Munition. Patent No. 286451, 14 May 2024.
74. Martel, R. Rocket Propelled Drone. U.S. Patent Application US20210031913A1.